Stability analysis of branched silver electrodeposits: Solid phase growth under a marginally stable regime

M. A. Pasquale, S. L. Marchiano, P. L. Schilardi, R. C. Salvarezza, and A. J. Arvia*
Instituto de Investigaciones Fisicoquimicas Teóricas y Aplicadas (INIFTA) (UNLP-CONICET), Sucursal 4, Casilla de Correo 16, (1900) La Plata, Argentina

(Received 30 August 2001; revised manuscript received 5 December 2001; published 8 April 2002)

The mass-transport controlled growth of silver deposits at the early stage of multiple bump formation, and when a silver single needle growth regime is attained, are investigated. Linear stability analysis as proposed by Barkey, Muller, and Tobias [J. Electrochem. Soc. **136**, 2199 (1989)] is applied to kinetic mesoscale data. A reasonable correlation between the current density and the average amplitude of unstable perturbation is established.

DOI: 10.1103/PhysRevE.65.041608 PACS number(s): 81.15.Pq, 61.43.Hv, 68.35.Rh, 68.55.Jk

The kinetics and mechanism of metal electrocrystallization are sensitive to the nature of the substrate surface, i.e., the predominant crystalline face, the type and density of surface defects, the composition of the electrolyte solution, including impurities, and the operation conditions, i.e., the characteristics of either the current or the potential routine applied to the electrochemical interface. These routines and the cell design, including hydrodynamic conditions, determine either the current or the electric potential distribution at the reaction front [1–3].

Frequently, the growth mode of metal electrodeposits is investigated by analyzing the features of growth patterns produced using quasi-bi-dimensional (quasi-2D) electrochemical cells with either a concentric or a parallel cathode-anode arrangement accommodated between flat transparent plates of insulating material to visualize the growing process [4–13]. In general, these growth patterns may be described as a set of branches either with or without tip splitting. For the latter, each branch shows a principal axis in the fastest growth direction, a tip with a stable shape associated with the fastest moving front, and a stem from which secondary branches could emerge. The tip remains either quasistable in shape at least from the μm scale upwards, as can be observed for dendrites and whiskers. Conversely, tip growth may exhibit spontaneous, either periodic or random, splitting as results from diffusion-limited aggregation [1–3]. The occurrence of a particular growth mode can be predicted by the stability theories on the basis of a set of parameters related to the concentration overpotential at the surface of the growing deposit, the activation overpotential including the influence of lattice properties, and the ohmic overpotential [14–22]. This issue is important in dealing with a quantitative theory for roughness development in metal electrodeposition [22,23]. Several electrochemical and hydrodynamic parameters influence roughness characteristics, such as differences in the growth rate between crystal phases [23,24], mass transport effects related to instability of the surface with respect to perturbation in shape [22,25,26], and the natural convection contribution to mass transfer rate from the solution to the growing front, which may interact with the development of surface features [27–29].

This paper refers to the mass transport controlled growth of silver deposits under two limiting situations, namely, at the early stages of multiple bump formation, and when a silver single needle growth regime is attained. Kinetic mesoscale data derived from sequential imaging offer the possibility of applying the linear stability analysis proposed by Barkey, Muller, and Tobias [22] and to establish a reasonable correlation between the current density and the average amplitude of unstable perturbations.

The experiments, which were run with a circular and a rectangular quasi-2D cell, are described elsewhere [30,31]. These cells consisted of two parallel glass plates separated by the distance $l_s = 0.05$ cm. The circular cell, principally used to follow the development of whiskers, involved a concentric electrode arrangement, i.e., a platinum wire (99.99% purity, radius 0.035 cm) cathode placed at the center of the cell, and a silver ring anode (99.99% purity, radius $r_a = 5$ cm). The rectangular cell, which was more adequate to observe the early stage of growth, consisted of two silver wire electrodes (99.9% purity, radius $r_0 = 0.025$ cm, wire length $l_w = 2.85$ cm) with $l_s = 0.05$ cm and a cathode-to-anode separation $l_{a\text{-}c} = 1.90$ cm. Both cell designs initially favored a homogeneous primary current distribution. Both cells were mounted on a suspended table to avoid any influence of spurious mechanical vibrations on the electrochemical processes [30,31].

Aqueous 2.4×10^{-2} M silver sulfate prepared from Milli-Q* water and analytical reagent grade chemicals, and saturated with purified nitrogen was utilized as working solution. Runs were made at 298 K.

Silver electrodeposition was performed by applying an anode-to-cathode potential difference ($\Delta E_{a\text{-}c}$) selected in the range where there was no interference by the hydrogen evolution reaction. During the electrodeposits growth a sequence of photographs at different electrolysis time (t) was taken, and simultaneously cathodic current (I_c) transients were recorded. The degree of reproducibility of each set of data was carefully checked by repeating each run at least three times.

Morphological details of silver electrodeposits at the end of each run were obtained from scanning electron micro-

*Corresponding author. Fax: 54-221-425-4642; Email address: ajarvia@inifta.unip.edu.ar

graphs (SEM). For this purpose, each specimen was fixed to the sample holder using a small amount of silver paint.

The process of silver electrocrystallization takes place in aqueous solutions through the following overall process:

$$\mathrm{Ag}^{+}(\text{aqueous}) + e^{-}(\text{cathode}) = \mathrm{Ag}^{+}(\text{crystal}) + e^{-}(\text{conduction band}). \quad (1)$$

The exchange current density j_0 of reaction (1) is strongly dependent on the crystallographic phases, their distribution, and the existence of surface defects [32–35]. For stepped polycrystalline silver in aqueous 1 M silver sulfate at 298 K, the value of $j_0 = 24 \pm 5$ A/cm^2 has been reported [36]. Accordingly, reaction (1) on stepped polycrystalline silver surfaces can be considered as one of the fastest, most electrochemically reversible interfacial processes. Silver electrodeposition at the single tip as well as the origin of instabilities leading to branching are controlled by diffusion, as in the case of microelectrodes [37] and branched metal electrodeposition in a 50-μm gap cell [38,39]. In these cases, the interface moves so slowly that it remains effectively stationary during the time needed for relaxation of the diffusion field.

The polarization curves were obtained at the rate 0.2 V/s to diminish the influence of surface roughness of the growing electrodeposit on the current response. They are plotted [Fig. 1(a)] as either $\Delta E_{a\text{-}c}$, the anode-to-cathode potential difference, or $\Delta E'_{a\text{-}c}$, the value of $\Delta E_{a\text{-}c}$ after ohmic drop correction, versus I_c. The linear stability analysis was performed for deposits grown at the ratio $j_c/j_{cL} = 0.28$, where j_c and j_{cL} are the cathodic current density and limiting current density, respectively. This ratio results when $\Delta E_{a\text{-}c} = -0.38$ V ($\Delta E'_{a\text{-}c} = 0.04$ V), a potential at which whisker formation can be observed.

The early stages of growth [Figs. 1(b)–1(c)] are characterized by the formation of a granular structure consisting of regularly distributed bumps 12 ± 2 μm in average size, and 28 ± 5 μm interbump average separation distance. The average time for the development of these bumps is about 10 s. The second stage [Fig. 1(c)] involves the triggering of many trees resembling the morphology predicted by the diffusion limited aggregation model [1–3] [Fig. 1(c)]. Finally, one of the branches originates a single needle branch (whisker) [Fig. 1(d)] that tends to dominate the growth pattern. The whisker shows a parabolic needle with a local tip radius 2.5 ± 0.5 μm and length 30 ± 1 μm. Occasionally, single needle formation may be accompanied by a quasiparallel lateral secondary branching on the stem surface starting from a certain distance from the tip downwards. As t increases, a little thickening of lateral branches increasing in going from the tip downwards is observed. The axial growth rate of the whisker is about two orders of magnitude larger than that in the transversal direction.

SEM micrographs show that the topography of needle tips [Fig. 2(a)] consists of stepped terraces and cavities 0.11 ± 0.01 μm^2 in average area covered by small crystals 0.020 ± 0.005 μm in average height and 0.38 ± 0.05 μm average intercrystal separation. As seen from the tip profile [Fig.

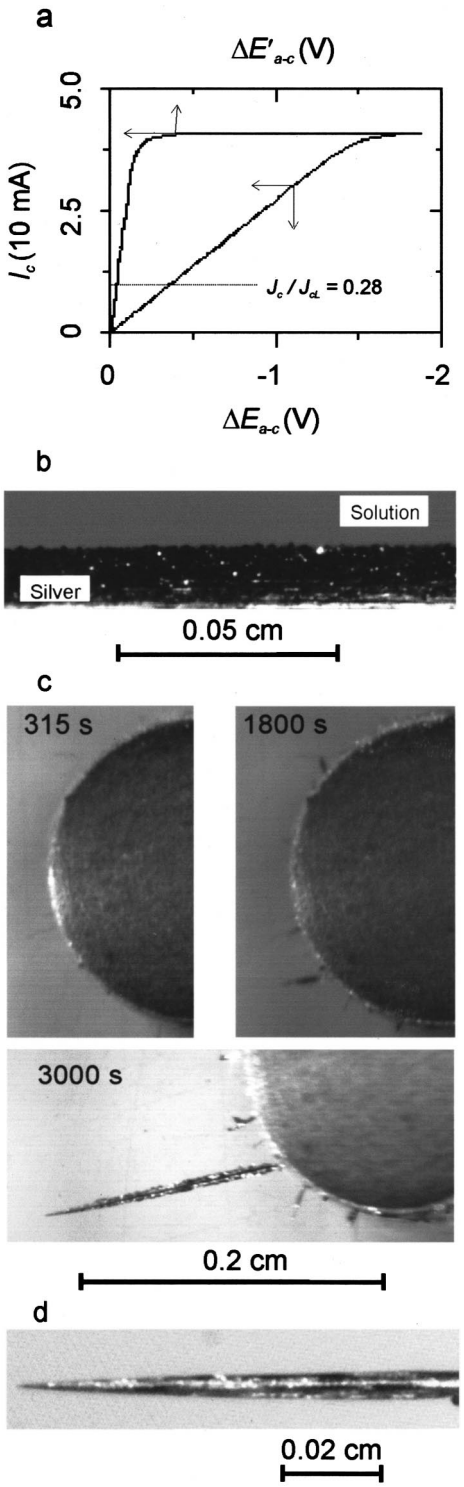

FIG. 1. (a) Polarization curve recorded at 0.2 V/s both without (I_c vs $\Delta E_{a\text{-}c}$) and after ohmic drop correction (I_c vs $\Delta E'_{a\text{-}c}$). The horizontal line indicates $j_c/j_{cL} = 0.28$. (b) Profile of silver electrodeposit at the early stages of growth in the pseudo-2D rectangular cell; aqueous 0.024 M silver sulfate, $\Delta E_{a\text{-}c} = -0.380$ V, 298 K. Bump formation can be observed. (c) Sequential profiles of silver deposits produced using the pseudo-2D circular cell showing branching and whisker formation. (d) Needle portion of the whisker resulting at the end of the experiment shown in (c), $\Delta E_{a\text{-}c} = -0.380$ V.

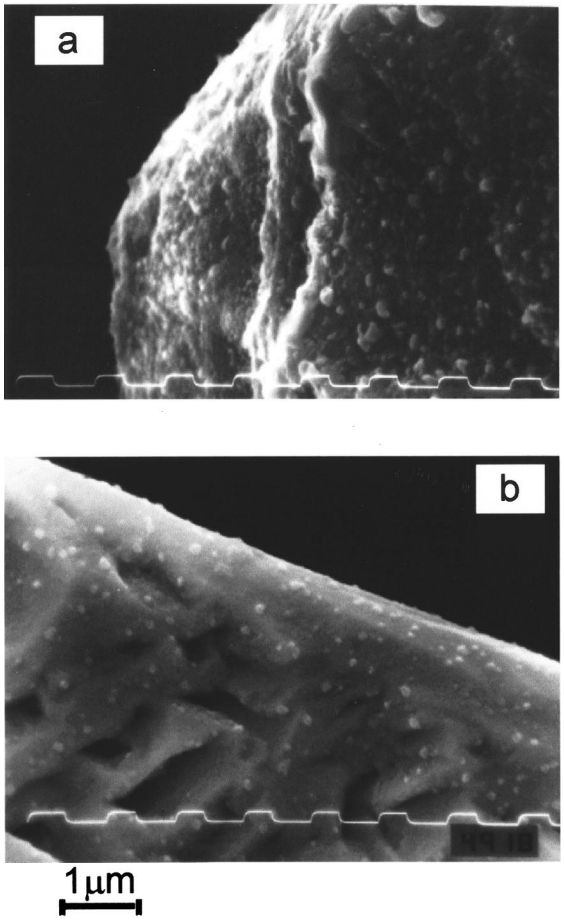

FIG. 2. SEM micrographs of different portions of a silver whisker produced in the pseudo-2D circular cell using aqueous 0.024 M silver sulfate, $\Delta E_{a\text{-}c} = -0.380$ V, 298 K. (a) tip portion, (b) lateral parabolic surface.

2(a)], most of these crystals appear as tiny pyramidal crystals with neither twining nor splitting. Their location fluctuates at random as they are continuously formed and disappear from the tip front as the latter advances into the solution. The upper limit for the half-life time of these crystals, estimated from the axial growth rate, $v = (1 \pm 0.1) \times 10^{-4}$ cm/s, and the average crystal height, is 2×10^{-2} s. Crystals and cavities of approximately the same size are also produced at the stem surface [Fig. 2(b)], although their number density is much smaller than at the needle tip.

Linear stability analysis based upon Mullins–Sekerka instability and underlying mechanism [40] has been applied to solidification phenomena [14–17,41] and metal electrodeposition [18–23,41]. For an interface subjected to a local disturbance of small magnitude, such as a local change in the surface roughness or in reactant concentration, it may react with either a stabilizing or a destabilizing response.

The stability theory formulated by Barkey, Muller, and Tobias a few years ago [22] accounts for ohmic potential, capillary, kinetic, and concentration overpotential, for a planar electrode surface. This theory shows a relationship between the rate of diffuison producing instabilities, i.e., the ratio j_c/j_{cL}, and the surface tension effect (capillary) producing smoothening. These two competing effects determine

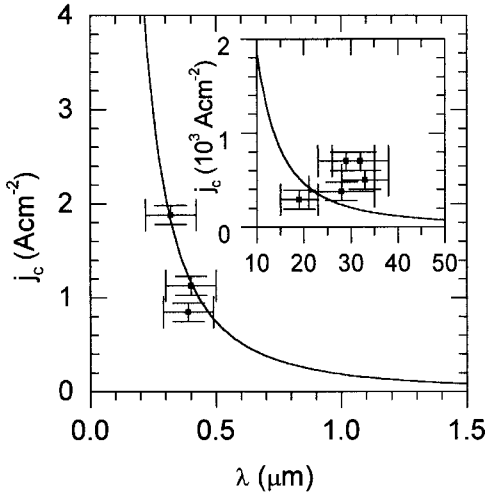

FIG. 3. Plot of j_c vs λ [Eq. (2)]. Data from whisker tips from three experiments. Inset: data from six experiments of unstable profiles. The marginally stable condition is determined by $j_c/j_{cL} = 0.28$. The solid curve corresponds to $j_c = 1.86 \times 10^{-9}/\lambda^2$. Error bars are shown.

the degree of stability of the growing system. When the capillary term is greater than the diffusion term, the system becomes stable, and when both effects are equal, the marginally stable condition is approached, as expressed by the equation

$$\frac{RTj_c}{n^2F^2Dc_b\left[1-\frac{j_c}{j_{cL}}\right]} = 8\pi^2\frac{\gamma v}{nF}\frac{1}{\lambda^2}, \tag{2}$$

where λ is the wavelength of the surface perturbation, v and γ are the molar volume and the surface tension, respectively, c_b is the concentration of silver ions in the bulk of the solution, D is the diffusion coefficient of silver ions in the solution, and $n=1$ is the number of electrons for a silver ion discharge; F and R are the Faraday and the universal gas constants, respectively. Note that for solids γ is a function of orientation with respect to the crystal axis [41]. However, the influence of surface tension anisotropy due to crystal orientation on a diffusion controlled electrochemical reaction at a polycrystalline solid involving a large value of j_0, can be neglected. Equation (2) plotted as j_c vs λ generates a family of curves, each one of them corresponding to a particular value of the ratio j_c/j_{cL}. The stability condition defined for a certain value of the ratio j_c/j_{cL} divides the j_c versus λ plane into one stability region located below and an upper instability one above the marginally stable condition for the growing system. Equation (2) was applied to the early stages of growth of silver electrodeposits (Fig. 3, inset) and to whisker tips (Fig. 3), taking $R = 8.31$ J/mol K; $F = 96\,500$ C/mol; $T = 298$ K; $\gamma = 1.1$ J/m^2; $c_b = 48$ mol/m^3; $D = 1.55 \times 10^{-9}$ m^2/s, $v = 1.03 \times 10^{-5}$ m^3/mol, and $j_c/j_{cL} = 0.28$.

For the early stages of growth, j_c and j_{cL} were obtained from the polarization curve and referred to the initial area of the cathode. The value of $\langle\lambda\rangle$, the average wavelength of instabilities, was taken as the average distance between the

bumps in the granular deposit, i.e., $\langle\lambda\rangle = 28 \pm 5$ μm. Data from different runs are included in the j_c vs $\langle\lambda\rangle$ plot (Fig. 3) as well as the functionality predicted by Eq. (2) for the marginally stable situation with $j_c/j_{cL} = 0.28$. As expected, data at the μm scale fall in the unstable region of the plot, i.e., under these conditions silver tree triggering is favored.

For the whisker tip approaching either a hemispherical or parabolic surface with a small radius of curvature, the value of j_c was calculated from the ratio $j_c = vF\rho/M = 1.3 \pm 0.5$ A/cm^2, where $v = (1 \pm 0.1) \times 10^{-4}$ cm/s is the axial growth rate determined from sequential photographs, $\rho = 10.5$ g/cm^3 and $M = 107.87$ are the density and molecular weight of silver, respectively. The average wavelength of instabilities, $\langle\lambda\rangle = 0.37 \pm 0.04$ μm, corresponds to the separation between unstable small crystals continuously growing and disappearing on the tip surface. These data fit Eq. (2) for the marginally stable situation. The validity of the j_c/j_{cL} ratio for both situations is consistent with the fact that the whisker tip behaves like a microelectrode in which the local ohmic overpotential becomes practically zero. From $j_c/j_{cL} = 0.28$, the value of j_{cL} for the whisker tip results in 4.6 ± 2 A/cm^2, a figure which is associated with an average diffusion layer thickness of 0.18 ± 0.08 μm. This value of the diffusion layer thickness indicates that small crystals 0.020 ± 0.005 μm in height are embedded in the diffuison layer around the tip.

Therefore, from the preceding examples it can be concluded that the stability theory offers a reasonable explanation for the development of silver whiskers and ramified electrodeposits covering a range of two orders of magnitude in the average instability wavelength scale.

The stability analysis of silver electrodeposits for two limiting situations, the initial growth of branching and the growth of whiskers, is considered. These deposits are produced from aqueous silver sulfate in quasi-2D cells, at 298 K.

Experimental data are analyzed using the stability theory described in Ref. [22]. The j_c vs λ^{-2} plot shows that data from the whisker tips fulfill the marginally stable condition, whereas those from branching initiation fall in the instability region in the plot.

This work was financially supported by PIP 4376 and PIP 0897 from Consejo Nacional de Investigaciones Cientificas y Técnicas (CONICET) and PICT 97-1993 from Agencia Nacional de Promoción Cientifica y Tecnológica of Argentina.

[1] P. Meakin, in *The Fractal Approach to Heterogeneous Chemistry, Surfaces, Colloids, and Polymers*, edited by D. Avnir (Wiley, London, 1990), Chap. 3.1.2, p. 131.

[2] *Solids Far From Equilibrium*, edited by C. Godrèche (Cambridge University Press, Cambridge, England, 1992).

[3] A. L. Barabasi and H. E. Stanley, *Fractal Concepts in Surface Growth* (Cambridge University Press, Cambridge, England, 1995).

[4] M. Matsushita, Y. Hayakawa, H. Honjo, and Y. Sawada, Phys. Rev. Lett. **53**, 286 (1984).

[5] M. Matsushita, Y. Hayakawa, and Y. Sawada, Phys. Rev. A **32**, 3814 (1985).

[6] D. G. Grier, E. Ben-Jacob, R. Clarke, and L. M. Sanders, Phys. Rev. Lett. **56**, 1264 (1986).

[7] Y. Sawada, A. Dougherty, and J. P. Gollub, Phys. Rev. Lett. **56**, 1260 (1986).

[8] S. D. G. Grier, D. A. Kessler, and L. M. Sander, Phys. Rev. Lett. **59**, 2315 (1987).

[9] F. Argoul, A. Arneodo, G. Grasseau, and H. L. Swinney, Phys. Rev. Lett. **61**, 2558 (1988).

[10] F. Argoul, A. Arneodo, J. Elezgaray, G. Grasseau, and R. Murenzi, Phys. Rev. A **41**, 5537 (1990).

[11] P. P. Trigueros, J. Claret, F. Mas, and F. Sagués, J. Electroanal. Chem. **312**, 219 (1991).

[12] A. Kuhn and F. Argoul, J. Electroanal. Chem. **397**, 93 (1995).

[13] P. Schilardi, S. L. Marchiano, R. C. Salvarezza, A. Hernández Creus, and A. J. Arvia, J. Electroanal. Chem. **431**, 81 (1997).

[14] J. A. McGeough and H. Rasmussen, J. Mech. Eng. Sci. **18**, 271 (1976); **19**, 163 (1977); **23**, 114 (1981).

[15] J. S. Langer, Rev. Mod. Phys. **52**, 1 (1980); Acta Metall. **25**, 1121 (1977).

[16] J. S. Langer and H. Mueller-Kumbhaar, J. Cryst. Growth **42**, 11 (1977).

[17] J. S. Langer, R. F. Sekerka, and T. Fujioka, J. Cryst. Growth **44**, 414 (1978).

[18] R. Aogaki, K. Kitazawa, Y. Kose, and K. Fukei, Electrochim. Acta **25**, 965 (1980).

[19] R. Aogaki and T. Makino, Electrochim. Acta **26**, 1509 (1981); J. Electrochem. Soc. **131**, 40 (1984).

[20] R. Aogaki, J. Electrochem. Soc. **129**, 442 (1982); **129**, 2447 (1982).

[21] U. Landau, EPRI Report No. EM-2393, 1982, unpublished.

[22] D. P. Barkey, R. H. Muller, and C. W. Tobias, J. Electrochem. Soc. **136**, 2199 (1989); **136**, 2207 (1989).

[23] D. P. Barkey, F. Oberholtzer, and Q. Wu, Phys. Rev. Lett. **75**, 2980 (1995).

[24] H. J. Pick, G. G. Storey, and T. B. Vaughn, Electrochim. Acta **2**, 165 (1960).

[25] N. Ibl and O. Dossenbach, in *Comprehensive Treatise of Electrochemistry*, edited by E. Yeager, J. O'M. Bockris, B. E. Conway, and R. Sarangapani (Plenum Press, New York, 1983), Vol. 6, Chap. 3, p. 133.

[26] B. Levich, *Physico-Chemical Hydrodynamics* (Prentice-Hall, Englewood Cliffs, NJ, 1962); J. S. Newman, *Electrochemical Systems*, 2nd ed. (Prentice-Hall, Englewood Cliffs, NJ, 1991).

[27] R. C. Alkire and D. B. Reiser, J. Electrochem. Soc. **131**, 2795 (1984).

[28] P. Carro, S. L. Marchiano, A. Hernández Creus, S. González, R. C. Salvarezza, and A. J. Arvia, Phys. Rev. E **48**, R2374 (1993); Fractals in the Natural and Applied Sciences **A41**, 191 (1994).

[29] P. Carro, S. Ambrosolio, S. L. Marchiano, A. Hernández Creus, R. C. Salvarezza, and A. J. Arvia, J. Electroanal. Chem. **396**, 183 (1995).

[30] P. L. Schilardi, G. Azzaroni, R. C. Salvarezza, and A. J. Arvia, Langmuir **15**, 1508 (1999); Phys. Rev. B **59**, 4638 (1999).

[31] A. S. M. A. Haseeb, P. L. Schilardi, A. E. Bolzan, R. C. V. Piatti, R. C. Salvarezza, and A. J. Arvia, J. Electroanal. Chem. **500**, 533 (2001).
[32] J. O'M. Bockris and A. K. N. Reddy, *Modern Electrochemistry* (MacDonald, London, 1970), Vol. 2, p. 125.
[33] E. Budevski, W. Bostanov, T. Vitanov, Z. Stoinov, A. Kotzewa, and R. Kaischev, Electrochim. Acta **11**, 1697 (1966).
[34] E. Budevski, W. Bostanov, T. Vitanov, Z. Stoinov, A. Kotzewa, and R. Kaischev, Phys. Status Solidi **13**, 577 (1966).
[35] J. D. Porter and T. O. Robinson, J. Phys. Chem. **97**, 6696 (1957).
[36] H. Gerischer and R. P. Tischer, Z. Elektrochem. **61**, 1159 (1957).
[37] R. M. Wightman and D. O. Wiepf, in *Electroanalytical Chemistry*, edited by A. J. Bard (Marcel Dekker, New York, 1989), Vol. 15, p. 267.
[38] C. Léger, J. Elezgaray, and F. Argoul, Phys. Rev. Lett. **78**, 5010 (1997).
[39] J. Elezgaray, C. Léger, and F. Argoul, J. Electrochem. Soc. **145**, 2016 (1998).
[40] W. W. Mullins and R. F. Sekerka, J. Appl. Phys. **34**, 323 (1963); **36**, 264 (1965).
[41] D. A. Kessler, J. Koplik, and H. Levine, Adv. Phys. **37**, 255 (1988).